Supporting information (SI) for

Ruthenium-based medium-entropy alloy oxide for hydrogen evolution linking to biomass sucrose upcycling

Gen Liu[a], Jingjing Yang[a], Wangxi Fan[a], Shuang Dong[b,*], and Zhou Yang[a,*]

[a.] Department of Chemistry and Chemical Engineering, Jiangsu University of Technology, Changzhou 213001, China.

[b.] School of Chemical Engineering and Materials, Changzhou Institute of Technology, Changzhou 213032, China.

*Correspondence: Zhou Yang, zhouyang@jsut.edu.cn. Shuang Dong, dongs@czu.cn.

Characterizations

The microstructure was observed by a field-emission scanning electron microscope (FE-SEM, Sigma 500), and transmission electron microscopy (TEM, JEM-2100) with selected area electron diffraction (SAED) and energy dispersive spectrometer (EDS). The chemical properties were scanned by X-ray diffraction (XRD, X'PERT POWDER, scanning rate is 10° min^{-1}) and X-ray photoelectron spectroscopy (XPS, ThermoFisher Scientific ESCALAB 250, Al target). The contents of Ru and Pd were tested by inductive coupled plasma-optical emission spectrometry (ICP-OES, Plasma 2000). The chemical product is characterized by ^{1}H nuclear magnetic resonance (NMR, Bruker Avance III HD, 400 MHz, solution is D_2O) and high-performance liquid chromatography (HPLC, Agilent 1260 series equipped with a UV detector, which was operated at 210 nm with Bio-Rad Aminex HPX-87H column at 50 °C, 5 mM of H_2SO_4 was used as the eluent with flow rate of 0.5 mL min^{-1}). The electrochemical measurements were performed by an electrochemical workstation (Chenhua, CHI 760E) including cyclic voltammetry (CV), linear sweep voltammetry (LSV), Chronopotentiometry (CP), electrochemical impedance spectroscopy (EIS), impedance-potential, and intensity-time (i-t) curve.

In the three-electrode system, 2 mg of sample was dispersed in 200 μL of mixed solution (deionized water: ethanol: Nafion = 2:7:1) to form ink, and then 10 μL of above ink was dripped on a glass carbon electrode (GCE) and dried at room temperature, which was used as the working electrode, and the Hg/HgO and graphite electrodes were used as the reference and counter electrodes, respectively. In the two-electrode system, the sample was fully mixed with acetylene black and polyvinylidene fluoride (PVDF) with a weight ratio of 8:1:1, and dispersed in appropriate N-methylpyrrolidone (NMP) to form slurry. The above slurry was coated on the nickel foam (1×1 cm) and dried. The test was performed in the C008-1 3H cell separated by the perfluorosulfonic acid proton exchange membrane.

The electrochemically active surface (ECSA) was calculated on the basis of the double-layer capacitance (C_{dl}) theory,[1]

$$ECSA = C_{dl} / C_s$$

Where the slope in the plot of current densities to scan rates stands for $2C_{dl}$, and C_s is 0.04 mF cm^{-2}.

Faradaic efficiency (*FE*), conversion, and selectivity of SOR

The half-reaction formula for product from SOR in 1 M KOH+0.1 M sucrose is listed as follows:

$C_{12}H_{22}O_{11} + 24OH^- \rightarrow 12HCOOH + 11H_2O + 24e^-$

FE of SOR is calculated based on the following equation:

$$FE\ (\%) = \frac{24 \times CHCOOH}{Q} \times V \times F \times 100\%$$

Where, C_{HCOOH} is the concentration (mol L^{-1}) of FA; V is the volume of tested electrolyte (10×10^{-3} L); F is the Faradaic constant (96485 C mol^{-1}); Q is the total charge (C) passed during electrochemical reaction.[2]

$$\text{Conversion } (\%) = 1 - \frac{nsucrose}{nsucrose0} \times 100\%$$

$$\text{Selectivity } (\%) = \frac{nHCOOH}{nproducts} \times 100\%$$

Where, $n_{sucrose}$ is the mol of sucrose, $n_{sucrose0}$ is the mol of original sucrose, n_{HCOOH} is the mol of FA, and $n_{products}$ is the mol of all products.

Supplementary figures

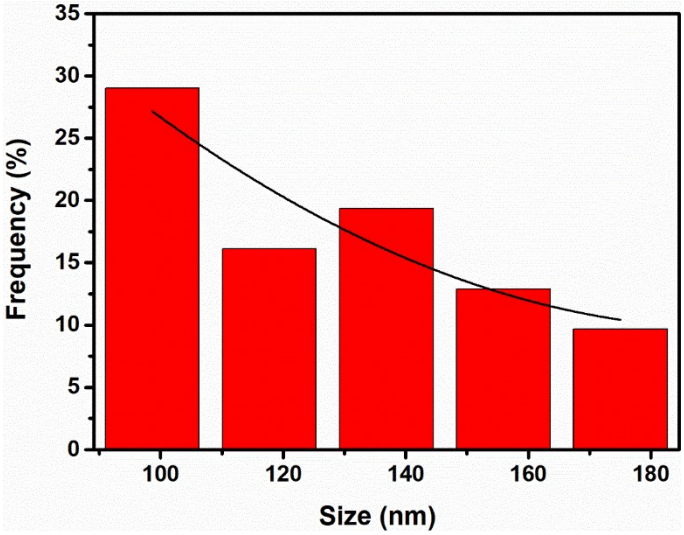

Fig. S1. Particle size distribution of $Ru_{0.5}Pd_{0.5}O_2$.

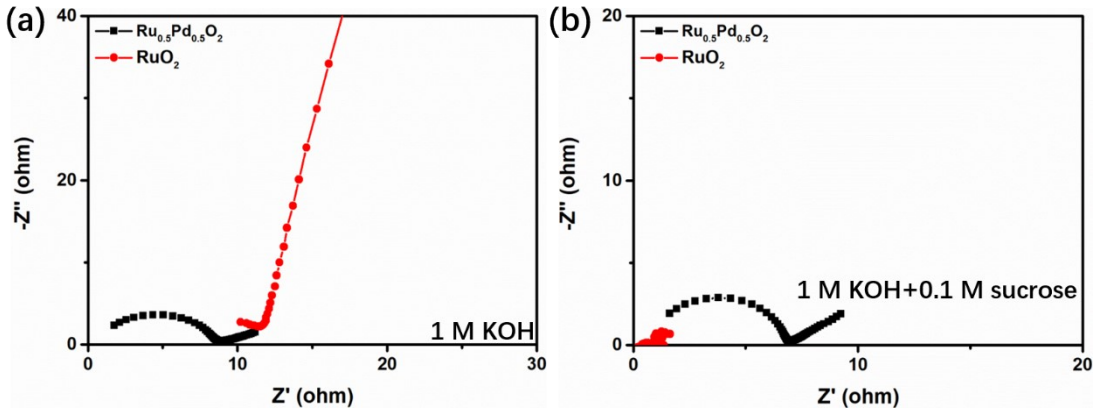

Fig. S2. EIS plots of $Ru_{0.5}Pd_{0.5}O_2$ and RuO_2 in (a) 1 M KOH and (b) 1 M KOH+0.1 M sucrose. (All the EIS test at Amplitude = 0.005 V from 1 HZ to 10^5 HZ).

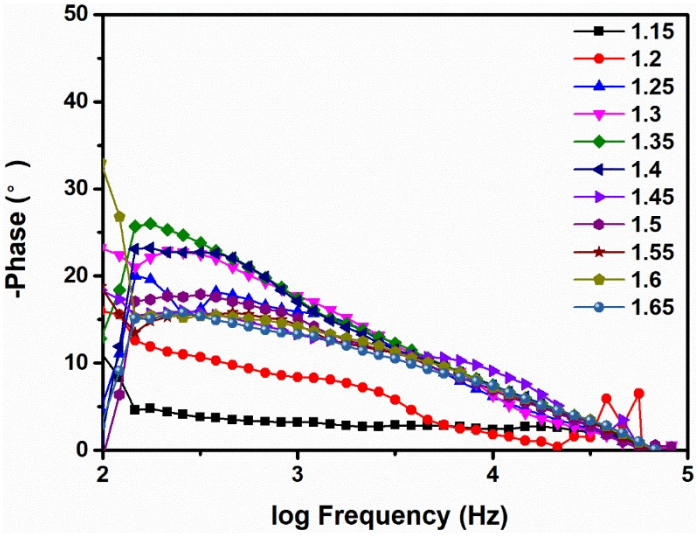

Fig. S3. *In-situ* bode plots of $Ru_{0.5}Pd_{0.5}O_2$ in 1 M KOH+0.1 M sucrose.

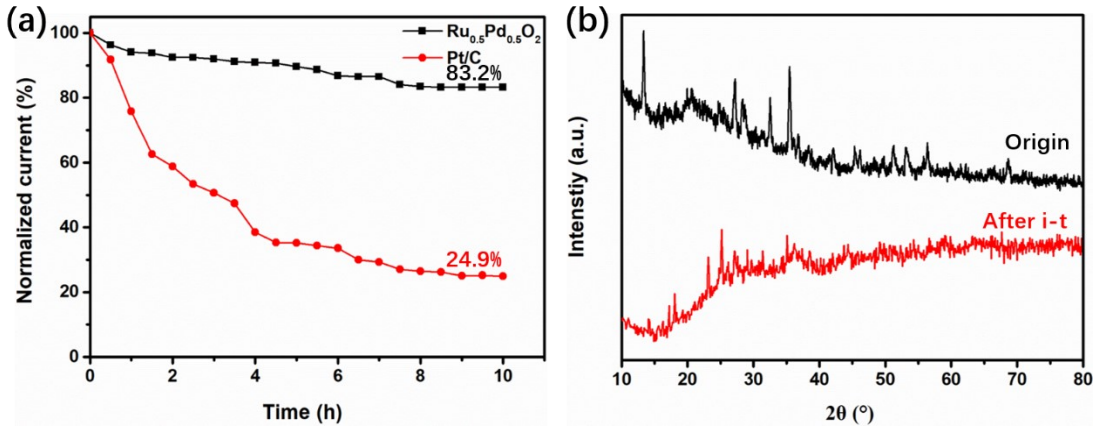

Fig. S4. (a) I-t plots of $Ru_{0.5}Pd_{0.5}O_2$ and Pt/C in 1 M KOH+0.1 M sucrose. (b) XRD pattern of $Ru_{0.5}Pd_{0.5}O_2$ after i-t test.

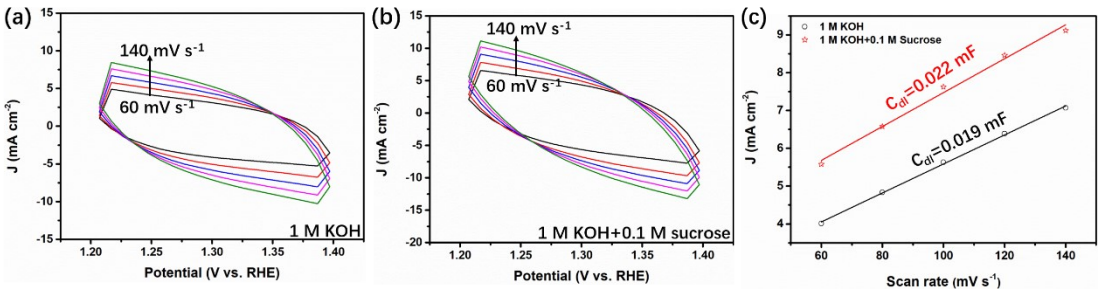

Fig. S5. CV curves at different scan rates of $Ru_{0.5}Pd_{0.5}O_2$ in (a) 1 M KOH and (b) 1 M KOH+0.1 M sucrose. (c) Plots of current density to scan rates.

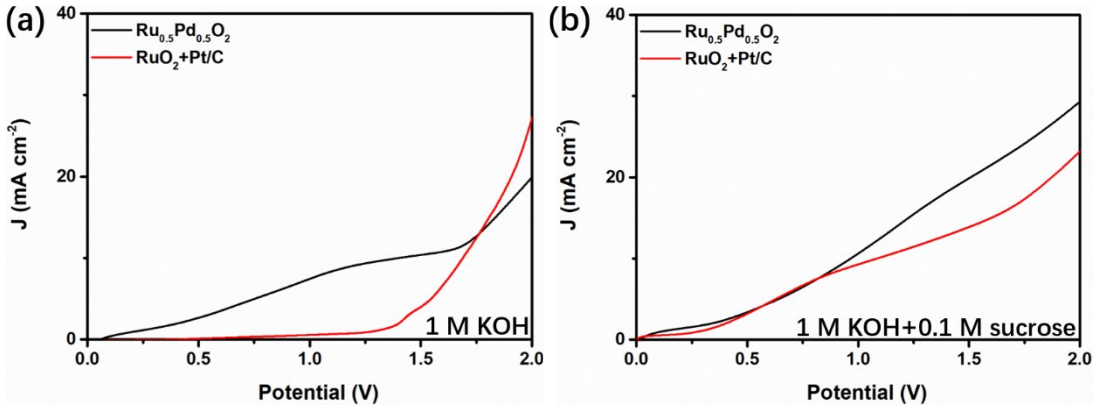

Fig. S6. Overall water splitting LSV curves of $Ru_{0.5}Pd_{0.5}O_2$ and RuO_2+Pt/C system in (a) 1 M KOH and (b) 1 M KOH+0.1 M sucrose.

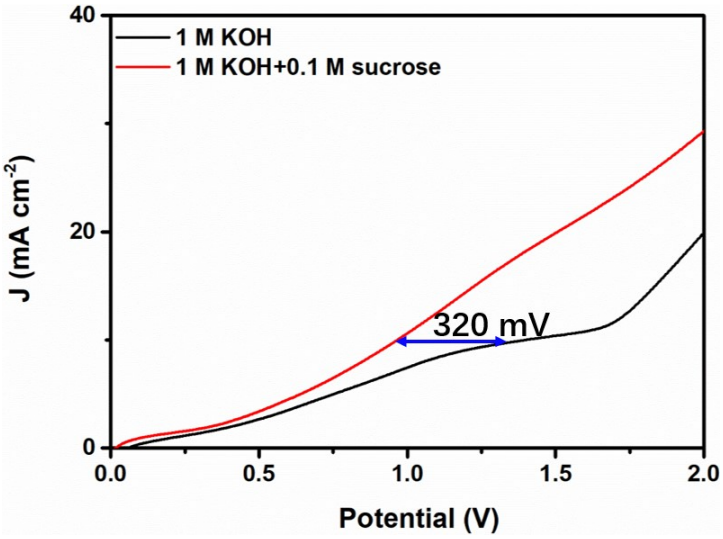

Fig. S7. Overall water splitting LSV curves of $Ru_{0.5}Pd_{0.5}O_2$ in 1 M KOH and 1 M KOH+0.1 M sucrose.

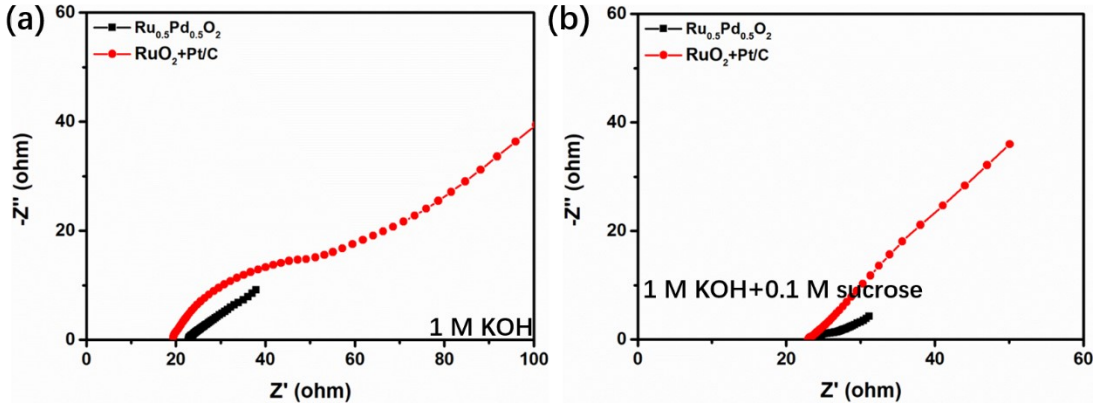

Fig. S8. EIS plots of $Ru_{0.5}Pd_{0.5}O_2$ and RuO_2+Pt/C system in (a) 1 M KOH and (b) 1 M KOH+0.1 M sucrose by the two-electrode method. (All the EIS test at Amplitude = 0.005 V from 1 HZ to 10^5 HZ).

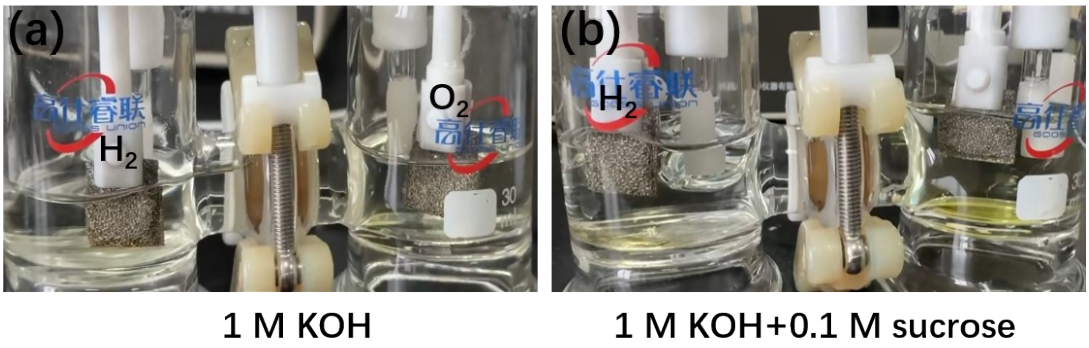

Fig. S9. Overall water splitting photos of $Ru_{0.5}Pd_{0.5}O_2$ loading on Ni foams in (a) 1 M KOH and (b) 1 M KOH+0.1 M sucrose.

Supplementary tables

Table S1. The contents of metals in the MEAO tested by ICP-OES

MEAO	Content of Ru (ppm)	Content of Pd (ppm)	Molar ratio of Ru to Pd
$Ru_{0.5}Pd_{0.5}O_2$	585.9	573.2	1.07

References

1. Z. Yang, H. Chen, M. Xiang, C. Yu, J. Hui and S. Dong, *Int. J. Hydrogen Energy*, 2022, 47, 31566-31574.
2. Y. Liu, Z. Chen, Y. Yang, R. Zou, B. Deng, L. Zhong, K. P. Loh and X. Peng, *Appl. Catal., B*, 2024, 331, 122559.